Structural Phase Transitions and Ionic Motions in Pyridinium Hexachlorotellurate(IV), Hexachlorostannate(IV), and Hexabromostannate(IV) Crystals as Studied by ^{1}H NMR

Yutaka Tai, Tetsuo Asaji, Ryuichi Ikeda*, and Daiyu Nakamura

Department of Chemistry, Faculty of Science, Nagoya University, Chikusa, Nagoya, Japan

Z. Naturforsch. **44 a**, 300–306 (1989); received January 21, 1989

The ^{1}H NMR second moment M_2 and the spin-lattice relaxation time T_1 are determined for pyridinium hexachlorotellurate(IV), hexachlorostannate(IV), and hexabromostannate(IV) at various temperatures above ca. 140 K. The phase transition temperatures already reported from halogen NQR experiments are determined as 272, 331, and 285 K, respectively, by differential thermal analysis (DTA). The DTA as well as differential scanning calorimetry measurements show that the above phase transitions are of second-order. For pyridinium hexachlorotellurate(IV) and hexabromostannate(IV), a sharp ^{1}H T_1 dip was observed at the transition temperature. This is interpreted in terms of a phenomenon related to the critical fluctuation of an order parameter. From the measurements of ^{1}H M_2, 60° two-site jumps (60° flips) around the pseudo C_6 axis of the cation are suggested to occur in the high temperature phases of the complexes. Modulation of X…^{1}H (X = Cl, Br) magnetic dipolar interactions due to the reorientational motion of the complex anions is considered as a possible relaxation mechanism in the high temperature phases.

Introduction

Recently, in the crystals of pyridinium hexachlorometallates(IV), $(C_5H_6N)_2MCl_6$ (M = Sn, Te, Pb, Pt) [1] and hexabromostannate(IV), $(C_5H_6N)_2SnBr_6$ [2] (hereafter $C_5H_6N^+$ is abbreviated to pyH^+) a structural phase transition was found from the temperature dependence of halogen NQR frequencies. The ^{1}H NMR spin-lattice relaxation time, T_1, determined for $(pyH)_2TeCl_6$ as a function of temperature shows a sharp dip at the transition temperature, T_c (= 273 K) [3]. This has been explained as ^{1}H relaxation modulated by the anion reorientation through dipolar relaxation of the second kind [4].

A previous powder X-ray diffraction study [1] has shown that the crystals of $(pyH)_2MCl_6$ (M = Sn, Te) in their high temperature phases are isomorphous. The accurate X-ray analysis of these complexes has revealed that the tin complex forms triclinic crystals with the space group $P\bar{1}$ ($Z = 1$) in the low temperature phase [1], while the high temperature phase of the tellurium complex is monoclinic, belonging to the space group B 2/m with $Z = 2$. Accurate structural data have not been reported as yet for the high temperature phase of the former complex and the low temperature phase of the latter. From a structural analysis of the high temperature phase of $(pyH)_2TeCl_6$, the most probable orientation of the cations was reported [5]: The nitrogen atom in pyH^+ was considered to occupy with equal probability the two neighbouring positions on the ring connected through the mirror plane of the crystal. The mirror plane is perpendicular to the ring plane and also one of the C–N bond and through its center. This is explainable by the presence of static or dynamic disorder for the pyridinium orientation in the crystal. Since ^{35}Cl NQR in $(pyH)_2TeCl_6$ was clearly observed at room temperature, static disorder, leading to a distribution of the electric field gradient formed at the chlorine nuclei and thus making difficult the observation of chlorine NQR signals, can be excluded. The ^{1}H T_1 and the ^{1}H NMR second moment, M_2, were measured to obtain more information about the cationic disorder and motional processes around the phase transitions in the complexes $(pyH)_2TeCl_6$, $(pyH)_2SnCl_6$, and $(pyH)_2SnBr_6$.

Experimental

The measurements of ^{1}H T_1 were carried out by means of homemade pulsed NMR spectrometers already described [6, 7] at three or four Larmor frequen-

* Institute for Molecular Science, Myodaiji, Okazaki 444, Japan.

Reprint requests to Prof. Dr. D. Nakamura, Nagoya University, Faculty of Science, Nagoya 464-01, Japan.

0932-0784 / 89 / 0400-0300 $ 01.30/0. – Please order a reprint rather than making your own copy.

Dieses Werk wurde im Jahr 2013 vom Verlag Zeitschrift für Naturforschung in Zusammenarbeit mit der Max-Planck-Gesellschaft zur Förderung der Wissenschaften e.V. digitalisiert und unter folgender Lizenz veröffentlicht: Creative Commons Namensnennung-Keine Bearbeitung 3.0 Deutschland Lizenz.

This work has been digitalized and published in 2013 by Verlag Zeitschrift für Naturforschung in cooperation with the Max Planck Society for the Advancement of Science under a Creative Commons Attribution-NoDerivs 3.0 Germany License.

Zum 01.01.2015 ist eine Anpassung der Lizenzbedingungen (Entfall der Creative Commons Lizenzbedingung „Keine Bearbeitung") beabsichtigt, um eine Nachnutzung auch im Rahmen zukünftiger wissenschaftlicher Nutzungsformen zu ermöglichen.

On 01.01.2015 it is planned to change the License Conditions (the removal of the Creative Commons License condition "no derivative works"). This is to allow reuse in the area of future scientific usage.

cies between 10.5 and 33.5 MHz, employing the conventional $180°-\tau-90°$ pulse sequence. To obtain ^{1}H NMR M_2 values at various temperatures, ^{1}H resonance absorptions were recorded at 40 MHz by use of a JEOL JNM-MW-40 S broadline NMR spectrometer. During the measurements, the sample temperatures were controlled to within ± 0.5 K. The temperature were measured using copper–constantan thermocouples within an estimated accuracy of ± 1 and ± 3 K for the pulsed and broadline NMR experiments, respectively. X-ray powder patterns were recorded with a model VD-1A X-ray diffractometer from Shimadzu Co., equipped with a copper anticathode. The DTA experiments were done with a homemade apparatus already described [8]. For the measurements of differential scanning calorimetry (DSC), a Du Pont 990 thermal analizer was employed.

The crystals of $(pyH)_2TeCl_6$, $(pyH)_2SnCl_6$, and $(pyH)_2SnBr_6$ were prepared according to the method described in [2, 9] and purified by recrystallization from a hydrochloric or hydrobromic acid solution. The prepared samples were identified by conventional elementary analysis and by taking X-ray powder patterns, which were compared with those reported in [1, 2, 5].

Results

Figure 1 shows the temperature dependence of ^{1}H NMR M_2 determined for the powdered samples of $(pyH)_2TeCl_6$, $(pyH)_2SnCl_6$, and $(pyH)_2SnBr_6$. Below ca. 200 K, the complexes yielded a nearly constant M_2 of (5 ± 1) G^2. With increasing the temperature up to each T_{tr}, ^{1}H M_2 decreased to ca. 2 G^2. Above T_{tr}, the values of M_2 around 2 G^2 were almost temperature independent, although a gradual decrease in each M_2 could be observed.

When the temperature was increased and decreased in the DTA experiments, characteristic endo- and exothermic heat anomalies, respectively, with a long tail on the low temperature side were recorded for all complexes studied. The peak temperatures of both anomalies were the same for these complexes. For crystals showing this kind of heat anomalies we have assigned the peak temperature to T_{tr}, referring to experimental evidences already reported [10]. For the crystals of $(pyH)_2TeCl_6$, $(pyH)_2SnCl_6$, and $(pyH)_2SnBr_6$, therefore, T_{tr} was determined as 272, 331, and 285 K, respectively.

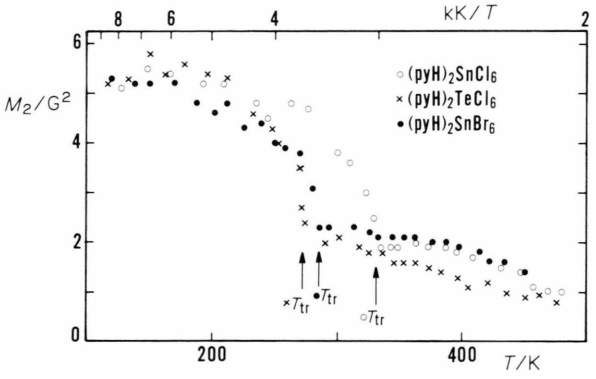

Fig. 1. Temperature dependence of the ^{1}H NMR second moment M_2 observed for powdered samples of pyridinium hexachlorotellurate(IV), hexachlorostannate(IV), and hexabromostannate(IV).

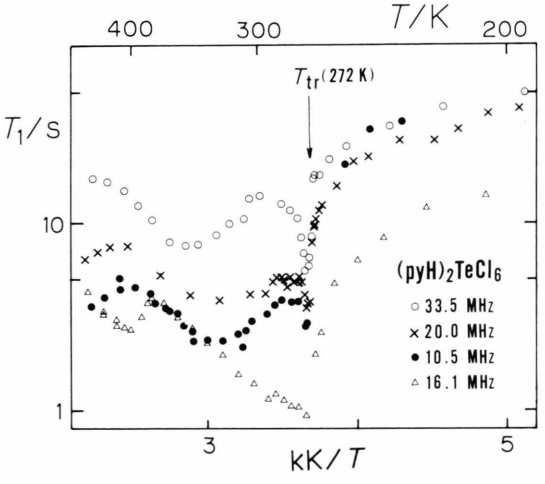

Fig. 2. Temperature variation of ^{1}H NMR spin-lattice relaxation times T_1 determined at four Larmor frequencies for a powdered sample of pyridinium hexachlorotellurate(IV).

The temperature variations of ^{1}H T_1 determined at the Larmor frequencies chosen between 10.5 and 33.5 MHz are shown in Figs. 2, 3, and 4 for $(pyH)_2TeCl_6$, $(pyH)_2SnCl_6$, and $(pyH)_2SnBr_6$, respectively. As for $(pyH)_2TeCl_6$ and $(pyH)_2SnCl_6$, a slightly nonexponential recovery of the magnetization was observed in the low temperature phase as well as in a limited temperature range in the high temperature phase when the Larmor frequency around 16–20 MHz was employed. In this case, the T_1 values were estimated by approximating the magnetization recovery to the exponential one. Preliminary results of ^{1}H T_1 obtained for $(pyH)_2TeCl_6$ were already reported as a

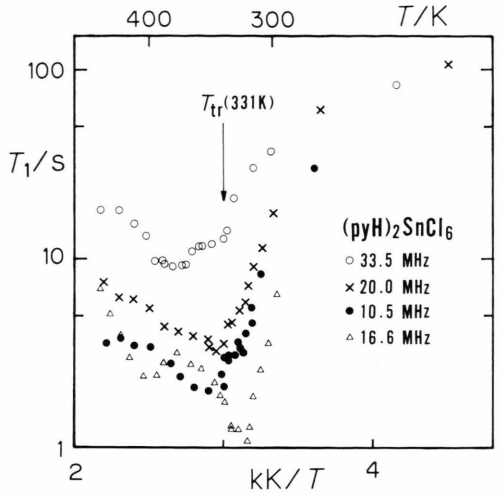

Fig. 3. Temperature variation of ^{1}H NMR spin-lattice relaxation times T_1 determined at four Larmor frequencies for a powdered sample of pyridinium hexachlorostannate(IV).

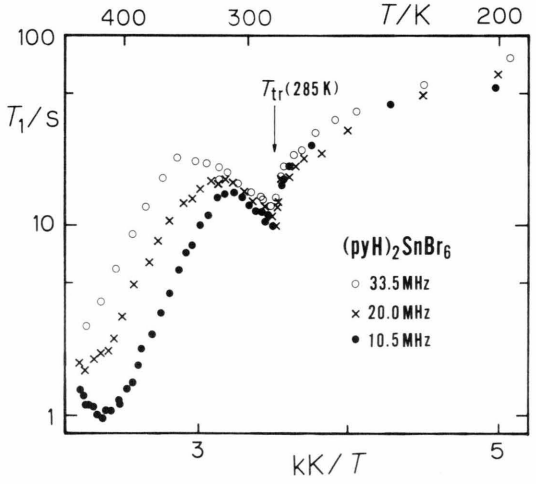

Fig. 4. Temperature variation of ^{1}H NMR spin-lattice relaxation times T_1 determined at three Larmor frequencies for a powdered sample of pyridinium hexabromostannate(IV).

letter [3]. For $(pyH)_2TeCl_6$ and $(pyH)_2SnBr_6$, the log T_1 vs. T^{-1} curves obtained at each Larmor frequency yielded a sharp T_1 dip at T_{tr}. In the high temperature phase, shallow T_1 minima of 2.4 and 1.0 s for $(pyH)_2TeCl_6$ and $(pyH)_2SnBr_6$, respectively, were observed at the Larmor frequency of 10.5 MHz. For $(pyH)_2SnCl_6$, clear T_1 dips were not discernible at T_{tr}, probably because the temperature of the T_1 minimum of the high temperature phase is too close to T_{tr}.

Discussion

60° Two-Site Jump Model for the Motion of the Cation

X-ray diffraction studies have been carried out for $(pyH)_2SnCl_6$ [1] and $(pyH)_2TeCl_6$ [1, 5] in the low and high temperature phases. The X-ray powder patterns taken for the high temperature phase of both complexes could be interpreted as arising from isomorphous crystals. The crystal lattice of $(pyH)_2SnBr_6$ belongs to the space group B2 with $Z=2$ at room temperature [2], and the structure can be considered to be close to that of $(pyH)_2TeCl_6$. This indicates that almost the same arrangement of cations in the crystals can be expected in the high temperature phases of these complexes.

As the most probable motional mode of the cation occurring in the high temperature phase, we assumed 60° flips of the whole cation about its pseudo C_6 axis. This is because the cationic ring can be regarded to be planar, and the disordered cationic orientations concluded from the X-ray study on $(pyH)_2TeCl_6$ [5] can be superimposed by this mode. ^{1}H M_2 values for the rigid lattice and those averaged over the above motion were evaluated for each complex. For the calculation of ^{1}H M_2, the coordinates of the heavy atoms determined at room temperature were used for both the high and low temperature phases of each complex studied. The protons in a pyH^+ ring were assumed to be located on the line connecting the center of the ring with the respective ring atom. The center of the cationic ring in each complex was evaluated by taking the average of the coordinates of the six heavy atoms determined by the X-ray studies. The C–H and N–H distances were taken to be equal and set at 1.06 Å.

The ^{1}H M_2 values were calculated by taking ^{1}H...^{1}H dipolar interactions into account, resulting from all protons in the 7^3 primitive cells around the resonant protons for each complex. A program PYM 2 written by us [11, 12] was employed for the calculation at Nagoya University Computation Center. The calculated and observed M_2 values are listed in Table 1.

The M_2 values observed above T_{tr} for the present complexes can be fairly well interpreted by the 60° two-site jump model for the motion of the pyridinium cation. However, partial excitation of six-site reorientations about the pseudo C_6 axis cannot be excluded in the high temperature phases of these complexes if one considers that the M_2 values observed at high temperatures were small compared with those calcu-

Table 1. The calculated and observed ^{1}H NMR M_2 values for pyridinium hexachlorotellurate(IV), hexachlorostannate(IV), and hexabromostannate(IV). The calculated intramolecular contributions are indicated in parenthesis. The phase transition temperature T_{tr} is given in the last column.

Compounds	$M_{2\,calc}/G^2$			$M_{2\,obs}/G^2$			
	rigid	60° two-site jump	C_6' reorientation *	120 ~ 200 K	just above T_{tr}	~450 K	T_{tr}/K
$(C_5H_6N)_2TeCl_6$	5.18 (3.86)	2.49 (1.67)	1.29 (0.96)	5.5 ± 1	2.2 ± 0.3	0.9 ± 0.1	272
$(C_5H_6N)_2SnCl_6$	5.26 (3.88)	2.57 (1.70)	1.31 (1.06)	5.3 ± 1	1.9 ± 0.3	1.4 ± 0.1	331
$(C_5H_6N)_2SnBr_6$	4.64 (3.41)	2.25 (1.49)	1.15 (0.85)	5.1 ± 1	2.3 ± 0.2	1.4 ± 0.1	285

* C_6' reorientation indicates the 60° reorientation about the pseudo C_6 axis of the cation.

lated based on the above motional mode. The observed M_2 values of the present complexes were decreased from ca. 200 K with increasing temperature, suggesting that the cations start the two-site jump motion considerably below T_{tr}.

Phase Transition Related to Cationic Two-Site Jump

According to the above discussion, the phase transition occurring in the present complexes should be of second order, characterized by the orientational order-disorder of the pyridinium cations. This interpretation is supported by the X-ray diffraction studies [1, 5] and the characteristic shapes of the DTA and DSC curves observed around T_{tr}. The transition entropy derived from the DSC measurements also supports this explanation. The fact that the transition entropy of ca. 5 J K^{-1}, roughly evaluated for the present complexes per 1 mol pyridinium ions, is approximately equal to $R \ln 2 = 5.8$ J K^{-1} mol^{-1}, supports the present two-site disorder model. The endothermic anomaly of the DTA and DSC curves, which started at temperatures much lower than T_{tr} and increased gradually with increasing temperature, conforms quite well with the gradual decrease of M_2 with increasing temperature in the low temperature phase. These results suggest the following mechanism of the phase transition. There exists a difference of lattice energies between two cationic orientations, namely, one is stable and the other is metastable in the low temperature phase. This difference decreases when the temperature approaches T_{tr} from the low temperature side and, above T_{tr}, these two orientations become equivalent.

For the two-site jump motion between nonequivalent sites, an extremely long ^{1}H T_1 minimum value has been derived theoretically and experimentally [13–15]. Provided that the correlation time τ of this jump motion is short enough around T_{tr} as compared with the inverse Larmor frequency employed, the T_1 due to this motion will stay extraordinally long in the whole temperature range. This is an explanation for the disappearance of the T_1 minimum corresponding to the gradual M_2 decrease of ca. 3 G^2 observed between ca. 200 K and T_{tr}.

The T_1 dips observed for $(pyH)_2TeCl_6$ and $(pyH)_2SnBr_6$ around T_{tr} were almost frequency independent. This can be explained by the fluctuation of lattice vibrations including the pyridinium cations expected to occur in the vicinity of the transition point [16]. In our previous letter on $(pyH)_2TeCl_6$ [3] we have tentatively assigned the ^{1}H T_1 dip to a motion of complex anions and the shallow T_1 minimum observed in the high temperature phase to the motion of the cation. However, we now propose a different interpretation for the ^{1}H T_1 of these complexes based on the newly obtained ^{1}H M_2 and ^{1}H T_1 data.

Modulation of X...^{1}H Magnetic Dipolar Interactions due to the Reorientational Motion of the Complex Anions

Our measurements of the quadrupolar spin-lattice relaxation time T_{1Q} of ^{35}Cl in $(pyH)_2SnCl_6$ showed that the reorientational motion of the anions occurs quite frequently in the high temperature phase [17]. Therefore, the modulation of X...^{1}H magnetic dipolar interactions due to the anionic reorientations can be considered as a possible relaxation mechanism for the protons in question. The existence of such a mechanism was reported for several complex compounds: $[C(NH_2)_3]_2PdCl_4$ [18], $(NH_4)_2PdCl_6$ [19], and $(NH_4)_2SnCl_6$ [20]. Applying this mechanism to the present complexes, we will quantitatively explain the observed shallow T_1 minima.

For the spin-lattice relaxation of ^{1}H nuclei (I-spins) through the nuclear magnetic coupling with quadru-

polar nuclei of chlorine or bromine isotopes (S-spins, having the spin quantum number S), one can obtain the following equations when the quadrupole coupling energy of S-spins is greater than their Zeeman energy [21]:

$$(T_1^{IS})^{-1} = \langle \gamma_I^2 \gamma_S^2 \hbar^2 S(S+1) \sum_{pairs} \{(1/12) K^{(-1,+1)} \cdot J(\omega_I - \langle \omega_S \rangle_a) + (3/2) K^{(1,0)} J(\omega_I) + (3/4) K^{(+1,+1)} J(\omega_I + \langle \omega_S \rangle_a)\} \rangle_b , \quad (1)$$

where

$$K^{(i,j)} = \langle |E^{(i,j)}|^2 \rangle_a - |\langle L^{(i,j)} \rangle_a|^2 , \quad (2)$$

$$J(\omega) = 2\tau_c/(1+\omega^2 \tau_c^2) . \quad (3)$$

Here, γ_I and γ_S denote the gyromagnetic ratio of ^{1}H and halogen nuclei, respectively, and ω_I and ω_S are their nuclear resonance angular frequencies under the weak field approximation for S spins. The square interaction amplitude $K^{(i,j)}$ is defined by (2) using the spatial parts $E^{(i,j)}$ of the dipolar Hamiltonian, which are given in [21] (see Appendix). The spectral intensity $J(\omega)$ is related to the correlation time τ_c for a fluctuation of X...^{1}H dipolar interactions through (3). The average $\langle \rangle_a$ means the motional average of I–S interactions for all interaction states appearing within a period of the order of ^{1}H T_1. The average $\langle \rangle_b$ takes into account the following ones: the average over crystallographically nonequivalent protons, the average over Zeeman splitted NQR lines of ^{35}Cl and ^{37}Cl for chloro complexes or ^{79}Br and ^{81}Br for the bromo complexes, and the powder average.

Since the halogen NQR frequencies [1, 2] are larger than the respective halogen NMR frequencies in the present study, (1) is considered to be applicable. The sum of the square interaction amplitudes $K^{(i,j)}$ was estimated under the following assumptions.

(i) A complex anion $[MX_6]^{2-}$ reorients isotropically among the six orientations corresponding to each M–X bond direction.

(ii) The electric field gradient tensor at a halogen nucleus X is axially symmetric about the M–X bond axis.

We calculated the contributions to ^{1}H T_1 from the interactions with the halogen nuclei within 5^3 primitive cells around the resonant proton at Nagoya University Computation Center using a computer program RELAX 4 written by us. The calculation is given in detail in the Appendix.

For $(pyH)_2SnBr_6$, the following relation holds for ^{1}H T_1 at a Larmor frequency of 10.5 MHz, because the bromine NQR frequencies are around 120 MHz [2]:

$$|\omega_I \pm \langle \omega_S \rangle_a| \gg \omega_I . \quad (4)$$

When this condition is satisfied, the T_1 minima due to $J(\omega_I \pm \langle \omega_S \rangle_a)$ and $J(\omega_I)$ may appear separately at different temperatures. Here, the T_1 minimum observed for $(pyH)_2SnBr_6$ was assumed resulting from $J(\omega_I)$ and was calculated as 0.6 s using

$$(T_{1\,min}^{IS})^{-1} = \langle \gamma_I^2 \gamma_S^2 \hbar^2 S(S+1) \sum_{pairs} \{(3/2) K^{(1,0)}/\omega_I\} \rangle_b = (3/2)(1/\omega_I) \gamma_I^2 \hbar^2 \cdot \langle \gamma_S^2 S(S+1) \rangle_S \langle \langle \sum_{pairs} K^{(1,0)} \rangle_{powd} \rangle_{proton} . \quad (5)$$

Here, $\langle \rangle_S$, $\langle \rangle_{powd}$, and $\langle \rangle_{proton}$ indicate the isotope average for two halogen isotopes of chlorine or bromine, the powder average, and the average over crystallographically nonequivalent protons, respectively. In the calculation, the position of the protons was assumed to be the same as that used for the M_2 calculation.

As for $(pyH)_2TeCl_6$, $\omega_I \pm \langle \omega_S \rangle_a$ and ω_I become of the same order of magnitude when the ^{1}H NMR frequency of 33.5 MHz is used. (The ^{35}Cl NQR frequencies are observed at ca. 16 MHz under zero magnetic field [1].) By assuming that the three terms in (1) give a single T_1 minimum at the same temperature, the lower limit of the T_1 minimum can be estimated to be about 3 s at 33.5 MHz.

The calculated T_1 minimum values of 0.6 and 3 s for $(pyH)_2SnBr_6$ and $(pyH)_2TeCl_6$, respectively, are of the same order of magnitude as the observed values, 1 s for $(pyH)_2SnBr_6$ (at 10.5 MHz) and 8 and 9 s for $(pyH)_2TeCl_6$ and $(pyH)_2SnCl_6$, respectively, at 33.5 MHz. These results strongly suggest that the motion of the complex anions is the most effective mechanism for yielding the minimum in the high temperature phase of the present complexes. A BPP type frequency dependence [13] of ^{1}H T_1 for $(pyH)_2SnBr_6$ observed above T_{tr} can be explained by use of the $J(\omega_I)$ terms in (1) under the condition of (4). Frequency dependences of ^{1}H T_1 for $(pyH)_2TeCl_6$ and $(pyH)_2SnCl_6$ are unexplainable by the simple BPP curve. This is because the first and third terms in (1) can no more be neglected if the ^{1}H NMR and chlorine NQR frequencies are of the same order as in the present study. Especially, when the ^{1}H NMR frequency is taken to be ca.

16 MHz near the chlorine NQR frequencies, the observed ^{1}H T_1 becomes very short suggesting the presence of a strong cross relaxation between the ^{1}H and chlorine nuclei, indicated by the first term on the right side of (1).

In the high temperature range above the T_1 minimum, ^{1}H T_1 of the hexachloro complexes still showed marked frequency dependences. These anomalous results seem to be due to the excitation of pseudo C_6 reorientation of the pyridinium cations.

Appendix

The following case was analyzed in detail by Kimmich [21]: The I-spins orient along the external magnetic field whereas the S-spins are approximately quantized along the principal axis of the electric field gradient (EFG) experienced. Therefore, two coordinate systems as shown in Fig. A1 were introduced.

The Z-axis of the I-system is directed along the external magnetic field, and the spin-spin vector r_{IS} is expressed in this system by the coordinates $(r_{IS}, \theta_I, \phi_I)$. The S-spins are quantized along the principal axis Z' of the EFG which is belonging to the S-system. In this system, r_{IS} can be expressed by the coordinates $(r_{IS}, \theta_S, \phi_S)$. The X- or Y-axis of the I-system and the X'- or Y'-axis of the S-system, having axially symmetric EFG, can be defined anywhere on the plane perpendicular to the Z- and Z'-axes, respectively. The intersect of these two planes (the line of nodes) is called A-axis. The B-axis is normal to the plane defined by the Z- and A-axes. By defining the Eulerian angles ξ, ε, ψ (Fig. A1), the S-system can be transformed to the I-system by use of the transformation matrix $R(\xi, \varepsilon, \psi)$ [22].

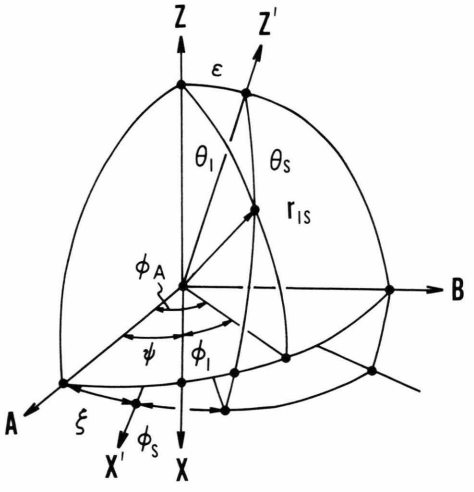

Fig. A1. The Zeeman coordinate system for I-spins and the electric field gradient coordinate system for S-spins. The I-spins and the S-spins are quantized along the Z- and Z'-axes, respectively. Eulerian angles ξ, ε, ψ, which transform the S-system to the I-system, are indicated. Spherical coordinates of the spin-spin vector r_{IS} are defined in each system.

The detailed expressions for the spatial parts $E^{(i,j)}$ of the dipole Hamiltonian are given in [21]. The components which appear in the T_1 formula (1) are written as follows:

$$E^{(-1,+1)} = r_{IS}^{-3}[-l_1 - m_2 - i(m_1 - l_2) + 3\sin\theta_I \sin\theta_S \exp\{-i(\phi_S - \phi_I)\}], \quad \text{(A1)}$$

$$E^{(1,0)} = r_{IS}^{-3}[-(l_3 - i m_3)/3 + \sin\theta_I \cos\theta_S \exp\{-i\phi_I\}], \quad \text{(A2)}$$

$$E^{(+1,+1)} = r_{IS}^{-3}[-\{l_1 - m_2 - i(l_2 + m_1)\}/3 + \sin\theta_I \sin\theta_S \exp\{-i(\phi_I + \phi_S)\}], \quad \text{(A3)}$$

where

$$\begin{pmatrix} l_1 \\ l_2 \\ l_3 \end{pmatrix} = \begin{pmatrix} \cos\xi\cos\psi - \sin\xi\cos\varepsilon\sin\psi \\ \sin\xi\cos\psi + \cos\xi\cos\varepsilon\sin\psi \\ \sin\varepsilon\sin\psi \end{pmatrix}, \quad \text{(A4)}$$

$$\begin{pmatrix} m_1 \\ m_2 \\ m_3 \end{pmatrix} = \begin{pmatrix} -\cos\xi\sin\psi - \sin\xi\cos\varepsilon\cos\psi \\ -\sin\xi\sin\psi + \cos\xi\cos\varepsilon\cos\psi \\ \sin\varepsilon\cos\psi \end{pmatrix}. \quad \text{(A5)}$$

Taking the arbitrariness of defining the X- and X'-axes into account, we averaged each term in (2) over all possible configurations before taking the motional average.

Since

$$(2\pi)^{-1}\int_{-\pi}^{\pi} E^{(-1,+1)}\,d\xi = (2\pi)^{-1}\int_{-\pi}^{\pi} E^{(1,0)}\,d\psi = (2\pi)^{-1}\int_{-\pi}^{\pi} E^{(+1,+1)}\,d\xi = 0, \quad \text{(A6)}$$

we have

$$K^{(-1,+1)} = \langle (2\pi)^{-2}\int_{-\pi}^{\pi}\int_{-\pi}^{\pi} |E^{(-1,+1)}|^2\,d\xi\,d\psi\rangle_a = \langle r_{IS}^{-6}[(1+\cos\varepsilon)^2 + 9\sin^2\theta_I\sin^2\theta_S - 6(1+\cos\varepsilon) f_+(\theta_I, \phi_A, \varepsilon)]\rangle_a, \quad \text{(A7)}$$

$$K^{(1,0)} = \langle (2\pi)^{-2}\int_{-\pi}^{\pi}\int_{-\pi}^{\pi} |E^{(1,0)}|^2\,d\xi\,d\psi\rangle_a = \langle |E^{(1,0)}|^2\rangle_a = \langle r_{IS}^{-6}[(1/9)\sin^2\varepsilon + \sin^2\theta_I\cos^2\theta_S - (2/3)\sin\theta_I\cos\theta_S\sin\phi_A\sin\varepsilon]\rangle_a, \quad \text{(A8)}$$

$$K^{(+1,+1)} = \langle (2\pi)^{-2} \int_{-\pi}^{\pi} \int_{-\pi}^{\pi} |E^{(+1,+1)}|^2 \, d\xi \, d\psi \rangle_a$$
$$= \langle r_{IS}^{-6} [(1/9)(1-\cos\varepsilon)^2 + \sin^2\theta_I \sin^2\theta_S$$
$$-(2/3)(1-\cos\varepsilon) f_-(\theta_I, \phi_A, \varepsilon)] \rangle_a . \quad (A\,9)$$

Here,

$$f_\pm(\theta_I, \phi_A, \varepsilon) = \sin^2\theta_I \cos^2\phi_A \pm \sin^2\theta_I \sin^2\phi_A \cos\varepsilon$$
$$\mp \sin\theta_I \cos\theta_I \sin\phi_A \sin\varepsilon , \quad (A\,10)$$

and ϕ_A denotes the azimuthal angle of r_{IS} in the ABZ coordinate system as shown in Figure A 1. The powder average of the contributions of $\sum_{\text{pairs}} K^{(i,j)}$ from halogen nuclei in 5^3 primitive cells was calculated with respect to each crystallographically nonequivalent proton.

[1] D. Borchers and Al. Weiss, Z. Naturforsch. **42a,** 739 (1987).
[2] K. B. Dillon, J. Halfpenny, and A. Marshall, J. Chem. Soc. Dalton Trans. **1985,** 1399.
[3] Y. Ito, T. Asaji, and D. Nakamura, phys. stat. sol. (a) **104,** K 97 (1987).
[4] M. O. Norris, J. H. Strange, J. G. Powles, M. Rhodes, K. Marsden, and K. Krynicki, J. Phys. **C 1,** 422 (1968).
[5] P. Khodadad, B. Viossat, P. Toffoli, and N. Rodier, Acta Cryst. **B 35,** 2896 (1979).
[6] L. S. Prabhumirashi, R. Ikeda, and D. Nakamura, Ber. Bunsenges. Phys. Chem. **85,** 1142 (1981).
[7] S. Gima, Y. Furukawa, R. Ikeda, and D. Nakamura, J. Mol. Struct. **111,** 189 (1983).
[8] Y. Kume, R. Ikeda, and D. Nakamura, J. Magn. Reson. **33,** 331 (1979).
[9] T. B. Brill and W. A. Welsh, J. Chem. Soc. Dalton Trans. **1973,** 357.
[10] D. Nakamura, J. Mol. Struct. **111,** 341 (1983).
[11] A. Kubo, M.Sc. Thesis, Nagoya University 1983.
[12] A. Kubo, R. Ikeda, and D. Nakamura, J. Chem. Soc. Faraday Trans. 2, **82,** 1543 (1986).
[13] G. Soda, J. Japanese Chem. **28,** 799 (1974).
[14] J. E. Anderson, J. Magn. Reson. **11,** 398 (1973).
[15] Y. Ito, T. Asaji, R. Ikeda, and D. Nakamura, Ber. Bunsenges. Phys. Chem. **92,** 885 (1988).
[16] M. E. Lines and A. M. Glass, Principles and Applications of Ferroelectrics and Related Materials, ch. 12, Clarendon Press, Oxford 1977.
[17] Y. Tai, A. Ishikawa, K. Horiuchi, T. Asaji, D. Nakamura, and R. Ikeda, Z. Naturforsch. **43a,** 1002 (1988).
[18] Y. Furukawa, S. Gima, and D. Nakamura, Ber. Bunsenges. Phys. Chem. **89,** 863 (1985).
[19] M. Bonori and M. Terenzi, Chem. Phys. Letters **27,** 281 (1974).
[20] J. H. Strange and M. Terenzi, J. Phys. Chem. Solids **33,** 923 (1972).
[21] R. Kimmich, Z. Naturforsch. **32a,** 544 (1977).
[22] H. Margenau and G. M. Murphy, The Mathematics of Physics and Chemistry, D. Van Nostrand, Amsterdam 1943.